

Release-Control Structures for Cantilever-Based Sensors

Behrouz Nikpour, Sasan Naseh, Leslie M. Landsberger*, Mojtaba Kahrizi,
Makarand Paranjape¹, Robert Antaki² and John F. Currie²

*Corresponding author: Department of Electrical and Computer Engineering,
Concordia University, Montréal, Québec, Canada H3G-1M8

¹Istituto per la Ricerca Scientifica e Tecnologica, Trento 38100, Italy

²Laboratory for the Integration of Sensors and Actuators,
Department of Engineering Physics, École Polytechnique de Montréal,
P.O.Box. 6079, Montréal, Québec, Canada H3C-3A7

(Received February 18, 1997; accepted February 4, 1998)

Key words: stressed oxide cantilever, anisotropic etching, use of fast-etch planes, release control, commercial CMOS

This paper concerns a cost-effective method of obtaining intact, released poly-in-oxide cantilever beams using bulk micromachining, within the constraints of simple post-processing of a standard CMOS fabrication sequence. An extension to the basic cantilever is used to prevent the main oxide/poly beam from bending upwards until the main cantilever is completely released from the underlying Si. This prevents a likely device failure mechanism. The cantilever and extension are designed based on etch anisotropy. The connection tethers joining the main cantilever with the extension can be set at an angle with respect to the underlying crystal structure such that the underetch rate of the etchant is high. The devices are fabricated using a standard commercially available CMOS process, and the beam-extension combination is released by postprocess anisotropic etching of silicon using TMAH. The devices are tested by applying known forces to the beam tips and determining the response of the piezoresistive poly element.

1. Introduction

The use of cantilever beams in microelectromechanical devices and systems is widespread and well documented. We describe a cost-effective design method for obtaining

intact released cantilever beams using simple postprocessing of a standard CMOS process.

Cantilever beam sensing elements are often made from stacked standard-process layers, including polysilicon and/or metal(s), imbedded between several SiO₂ dielectric layers. By the judicious placement of certain mask layers in a standard CMOS process, areas of exposed silicon substrate surrounding the perimeter of the intended cantilever can be readily defined.^(1,2) Thus-patterned wafers or die are then postprocessed in wet anisotropic etchant to sacrificially etch the silicon underneath the cantilever.

However, there are often different residual stresses present in the various layers which are commonly used as structural material for beams. Some of these stresses are impossible to avoid, such as the stress in thermally grown field oxides, while others are more readily controlled, such as those in CVD-deposited oxides. However, while microsystems technology is now able to produce flat dielectric cantilever beams by judicious control of the layers and their relative stresses, many commercial CMOS surface films are not designed for micromechanical applications. Thus, without this explicit stress control it might be impractical to implement certain structures in particular CMOS processes. Especially if high differential stresses exist between the as-fabricated layers (over which the designer has little or no control), the beam may bend severely during the release process. This may compromise the resulting device because the cantilever will bend diagonally from each of the two emerging free corners during the release process. If the bending is significant, it can induce cracks at the center of the cantilever as it is being released. Furthermore, if cracks occur during the release etch, imbedded polysilicon (poly) sensing elements sandwiched in the oxide cantilever would then be exposed to the silicon etchant, rendering the sensor nonfunctional.

In the interest of preventing this device failure mode without introducing additional complexity or constraints in the processing, we propose specially designed release-control structures. These extensions serve to prevent the structure from bending upwards until the main cantilever containing the polysilicon has been fully released from the bulk silicon underneath. In this way, the whole cantilever bends up only after the release-control extension has been completely released. The cracks in the cantilever, and therefore the damage to the imbedded poly lines, are thereby successfully eliminated. The release-control extension can remain as part of the cantilever mass, or it may be removed if necessary or appropriate. In this way, certain applications not needing high precision and in-plane cantilevers (for example, inertial sensors for toys), can be implemented at low cost in relatively inexpensive commercial CMOS processes not having low-stress dielectric layers. More generally, by using a technique such as this, the device designer does not need specific control of the stress in the CMOS layers.

The devices described by this paper are fabricated by a standard CMOS process, and the beams are released by postprocess anisotropic etching of silicon in TMAH. The devices are subsequently tested by applying known forces to the beam tips and measuring the change in resistance of the imbedded piezoresistive poly.

2. Background: Simple Cantilever without Extensions

Figure 1 illustrates a typical micromachined oxide cantilever structure fabricated on $\langle 100 \rangle$ silicon and having an imbedded polysilicon piezoresistor. After the beam is released via anisotropic etching, such a structure can act as an integrated sensor for accelerations perpendicular to the surface of the silicon. However, in actuality there is a problem in releasing this simple cantilever structure. This problem is caused by the residual stresses present within the films comprising the cantilever structures, inherent in the host process. The stresses are such that the structures tend to bend upwards out of the plane of the wafer. Figure 2 shows some intermediate stages that the structure attains during the release etch. Etching of the silicon under the cantilever begins at the convex corners where the fast-etching planes emerge (Fig. 2(a)). As etching continues, the silicon beneath the oxide obtains a sharp triangular profile (Fig. 2(c)). At this stage, the released part of the oxide bends upward because of internal stress in the field oxide. Since this bending occurs nonuniformly and from the two corners, severe deformations can occur where the two bends meet, i.e., above the sharp apex of the triangular shape. As etching proceeds, this sharp corner traces a line down the center of the cantilever and cracks occur in the oxide along this line (Figs. 2(c) and 2(d)). These cracks can leave the imbedded polysilicon exposed to attack by the silicon etchant. Clearly, this represents a catastrophic failure for the device. Our release-control extension was designed to alleviate this problem

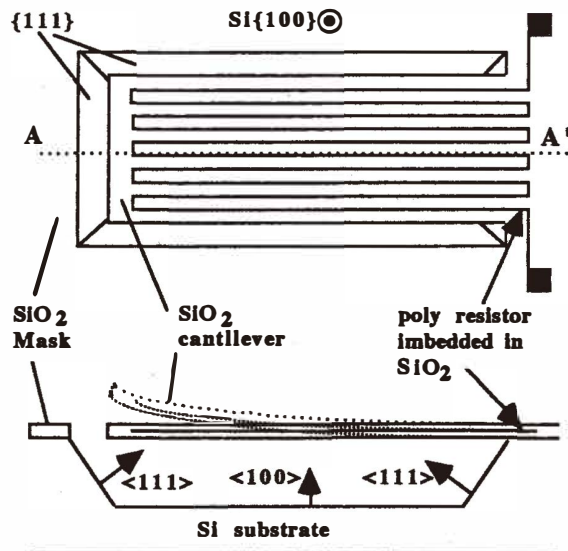


Fig. 1. Top and cross-sectional views of an oxide cantilever with imbedded polysilicon released by anisotropic etching of Si. If stressed, the oxide will bend upwards as shown.

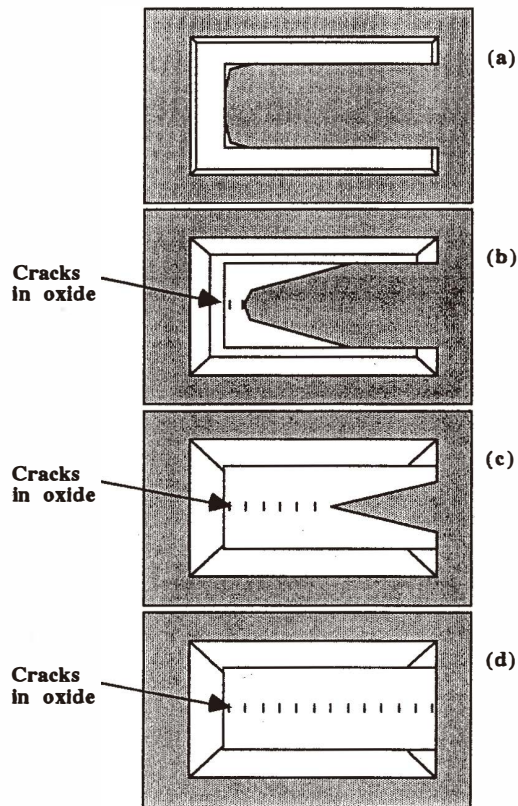


Fig. 2. Top view of a simplified cantilever structure. (a) After a short etch. (b) After an intermediate etch; bending and cracks have begun. (c) Almost released; with many cracks. (d) After the cantilever is completely released.

with a minimum of added complexity. A cantilever with an extension is schematically shown in Fig. 3.

3. Design of Release-Control Extension Structure

The extension was designed to keep the main cantilever flat until it is completely released from the underlying silicon. This is accomplished by setting the dimensions of the extension such that it becomes completely underetched only after the main cantilever has been completely released. In this way, the extension will hold down the main cantilever

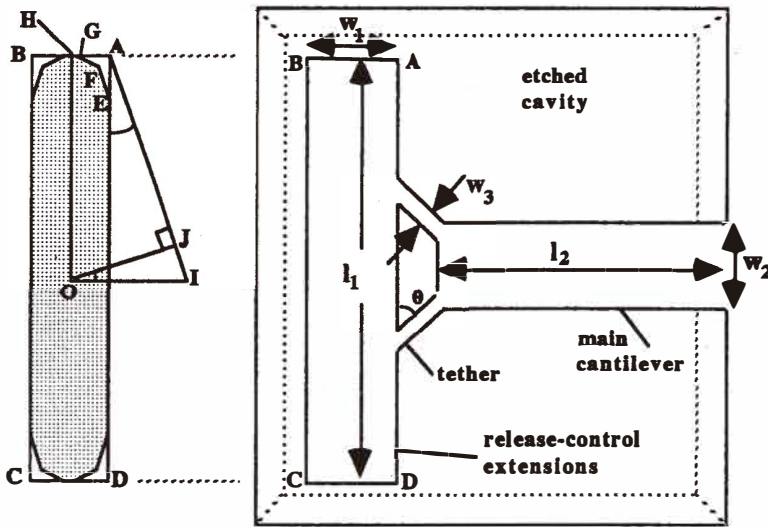


Fig. 3. Right: simplified schematic of a cantilever with a release-control extension. Left: schematic of features used to derive the time required to completely underetch a release-control extension.

(keep it flat) during the critical time when bending could cause damage.

In order for this method to be successful, detailed information on the etch anisotropy is required. For example, for the case of 25 wt% TMAH at 80°C, it is known from previous research^(3,4) that the angle at which mask undercut is fastest is 20–25° from the wafer flat (the wafer flat is <110>-oriented, 45° from the intersection of {111} planes with the wafer surface). The etch rate at this angle is approximately 2.2 times the etch rate at 45°. This angle varies little for TMAH at 15–25 wt% between 50°C and 90°C. For 5 wt% TMAH with a high dissolved silicon content (in order to protect Al pads in a CMOS process), this angle is close to 40–45° from the wafer flat.^(5–7) For a KOH-water solution, this angle would be about 30°⁽⁸⁾ from the wafer flat.

Figure 3 also shows the relevant parameters in the calculation of the time required to release the extension. The rectangular oxide extension ABCD is aligned with intersections of {111} planes and the wafer surface. Therefore, rapid underetching begins only at the convex corners, as depicted at corners A, B, C and D. Lines EF and FG indicate the emergent planes at corner A. After some time, the etch front FG will disappear and only EF will remain. Line AJI has been drawn parallel to EF. In order to completely underetch the rectangle ABCD, it is necessary for the etch front EF to travel a distance JO to reach point O. This distance can be calculated as follows:

$$JO = (IO)\cos(\angle JOI)$$

$$IO = [(AD/2) \tan(\angle IAD) + (AB/2)].$$

$$\begin{aligned} &\text{Since } \angle IAD = \angle JOI, \\ &JO = [AD \sin(\angle IAD) + AB \cos(\angle IAD)] / 2. \end{aligned}$$

By using the variables shown in Fig. 3, it can be seen that the time needed for release of the extension structure is

$$t_1 = [w_1 \cos \phi + l_1 \sin \phi] / 2E_\phi \quad (1)$$

where ϕ is the angle that the fastest underetching planes make with the wafer flat, and E_ϕ is the underetch rate at that angle. For example, in 25 wt% TMAH at 80°C, $E_\phi \sim 55 \mu\text{m/h}$ is the etch rate at the fastest etch angle of 24°^(3,4)

In order to calculate the time required to completely release the main cantilever, one must consider that first the tethers must be completely underetched before the convex corners of the main cantilever begin to be undercut. The time required to undercut the tethers is

$$t_2 = w_3 / 2E_\theta \quad (2)$$

where θ is the tether angle and E_θ is the etch rate at that angle. In order to minimize this time, t_2 , θ should be such that the tether is in a fast-undercutting configuration. While $\theta \sim 24^\circ$ is the optimum tether angle, angles in the range of $15^\circ < \theta < 45^\circ$ also give a satisfactorily low t_2 .

After the tethers are undercut, the time to release the main cantilever is given by

$$t_3 = [w_2 \cos \phi + 2l_2 \sin \phi] / 2E_\phi \quad (3)$$

Therefore, for a successful release operation such that the main cantilever is released before the extensions, $(t_2 + t_3)$ should be less than t_1 , that is, $(t_2 + t_3) < t_1$.

4. Device Fabrication and Testing

The devices having the following layer thicknesses were fabricated using a standard 1.5 μm commercial CMOS process:

- field oxide $\sim 0.9 \mu\text{m}$ thick,
- interpoly oxide $\sim 0.05 \mu\text{m}$ thick (under sensor poly),
- poly $\sim 0.3 \mu\text{m}$ thick,
- overlying CVD-deposited oxides totalling $\sim 2.1 \mu\text{m}$ thick,
- passivating nitride $\sim 0.5 \mu\text{m}$ thick.

The poly line was designed to be 2 μm wide and was folded 20 times on the main beam, such that the overall length of the sensing poly resistor was approximately 4,500 μm . Since the typical (nominal) sheet resistance of the poly was 20 $\Omega/\text{sq.}$, the expected resistance (R) was 45 k Ω .

The device dimensions were as follows.

- main cantilever length (l_2): 198 μm
- main cantilever width (w_2): 96 μm
- extension length (l_1): 1060 μm
- extension width (w_1): 60 μm
- tether width (w_3): 20 μm
- tether angle (θ): 40°

The die fabricated using the standard process was subsequently etched in TMAH to release the cantilever and extensions. Release etches were conducted in TMAH using a variety of compositions. For example, using the above dimensions, eqs. (2) and (3) indicate that in 25 wt% TMAH at 90°C, the main cantilever should be released in 1.5 h, and eq. (1) indicates that the extensions should be released 1.2 h later. Accordingly, a 3 h etch was sufficient to completely release both the cantilever and the extension in this example.

The devices were subjected to rudimentary electrical and mechanical tests, comparing their behavior before and after release. The end-to-end electrical resistances of the poly lines were measured by probing the aluminum bonding pads. The piezoresistive response of the devices was measured by applying known weights, from 0 to 40 mg, to the free end of the main cantilever, 10–15 μm from the tip end, using a profilometer.

5. Results and Discussion

Figures 4(a) and 4(b) show optical micrographs of the results of etched cantilevers with release-control structures. Figure 4(a) shows the tethered main cantilever after etching for 1 h in 25 wt% TMAH at 90°C. It is underetched to an extent between the conditions shown in Figs. 2(b) and 2(c). Since the micrograph is in total focus, it is clear that the cantilever is not bending upward at this release etch stage. It is also clear from the figure that the cantilever and imbedded poly lines are undamaged. Figure 4(b) shows the subsequently fully released cantilever. It has bent upward *after* full release of the main cantilever, and the imbedded poly lines are clearly undamaged by etching.

The end-to-end resistance (R) of poly lines was measured on 4 samples before etching and found to be 46.9 k Ω \pm 0.1 k Ω . This is well within the specifications published for the host CMOS process. After full release of the same samples by TMAH etching under the condition shown in Fig. 4(b), the vertical deflection of the tip of the main cantilever was measured to be approximately 20 μm , and R was measured to be 44.8 k Ω \pm 0.1 k Ω . Thus the after-etch deviation in resistance (ΔR) was 2.1 k Ω , and after-etch $\Delta R/R = 4.48\%$. Figure 5 shows the response of two different beams to the applied weights. In all cases, the deformation was proportional to the applied weight, ΔR was positive, and the maximum measured ΔR was 0.9 k Ω in response to a 40 mg applied weight.

The expected piezoresistive response and deflection of the beam obey the relations below. The relative change in poly resistance ($\Delta R/R$), in response to the strain in the poly layer and the vertical deflection of the beam tip (D), are given by⁽⁹⁾

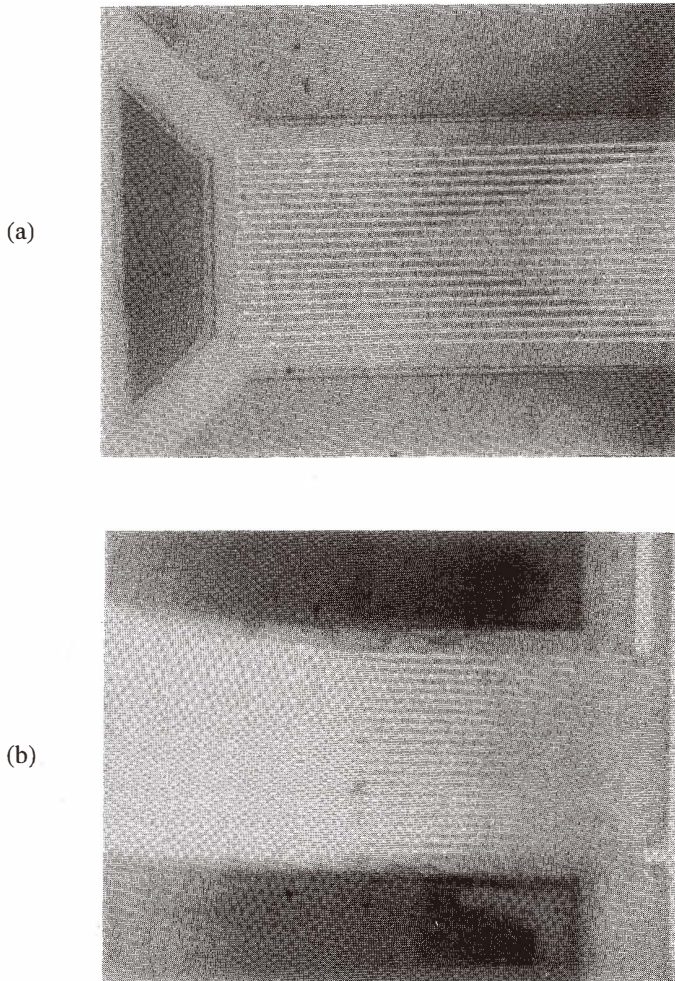


Fig. 4. Top views of a cantilever structure after etching in 25 wt% TMAH at 90°C: (a) the main cantilever and tethers after etching for 1 h; (b) the same main cantilever after full release. The poly lines are undamaged. Magnification = 200x.

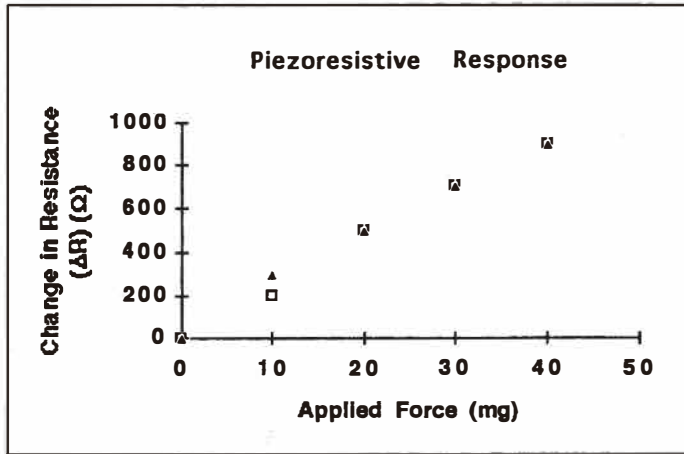


Fig. 5. Piezoresistive response of two beams under applied weights of 0–40 mg.

$$\Delta R / R = (G \times \sigma) = \frac{G \times (\text{applied load at beam tip}) \times (l_2) \times (y_{\text{neut}} - y_{\text{poly}})}{E_{\text{poly}} I_{\text{poly}} + E_{\text{nit}} I_{\text{nit}} + E_{\text{ox}} I_{\text{ox1}} + E_{\text{ox}} I_{\text{ox2}}}, \quad (4)$$

and

$$D = \frac{(1/3)(\text{applied load at beam tip})(l_2)^3}{(E_{\text{poly}} I_{\text{poly}} + E_{\text{nit}} I_{\text{nit}} + E_{\text{ox}} I_{\text{ox1}} + E_{\text{ox}} I_{\text{ox2}})}, \quad (5)$$

where G is the gage factor of the polysilicon, σ is the strain in the polysilicon, E_{ox} , E_{nit} and E_{poly} , are Young's modulus of each layer, and I_{ox1} , I_{poly} , I_{ox2} and I_{nit} are the second moments of inertia of each layer about the beam's neutral axis (y_{neut}).⁽⁹⁾ Using the device dimensions given above and the mechanical constants given below, y_{neut} was calculated to be $2.28 \mu\text{m}$ from the bottom of the beam, approximately $1.18 \mu\text{m}$ above the middle of the poly layer (y_{poly}).

- Young's modulus of polysilicon: $E_{\text{poly}} = 1.5 \times 10^{11} \text{ N/m}^2$ ⁽¹⁰⁾
- Young's modulus of silicon dioxide: $E_{\text{ox}} = 0.73 \times 10^{11} \text{ N/m}^2$ ⁽¹¹⁾
- Young's modulus of silicon nitride: $E_{\text{nit}} = 3.8 \times 10^{11} \text{ N/m}^2$ ⁽¹¹⁾

Mechanical constants for CMOS process layers, such as G , E_{ox} , E_{nit} and E_{poly} , can vary with the fabrication conditions. For example, values of G between -15 and -25 have been reported for n-type polysilicon.⁽¹²⁾ For the cantilevers reported in this paper, the after-etch deflection ($20 \mu\text{m}$) and ΔR ($2.1 \text{ k}\Omega$) were found to correspond to $G = -15$, calculated using the above equations. The measured ΔR of $0.9 \text{ k}\Omega$ in response to a 40 mg applied weight

was found to be consistent with $G = -15$ and the above equations.

If appropriate, the extensions can be removed by simple mechanical force. In the devices fabricated in this work, the extensions were easily broken off by applying a force of approximately 10 mg near the center of the release-control extension.

6. Conclusion

Effective release-control structures for commercial CMOS-based cantilever microsensors were designed by taking into account the precise anisotropy of the etchant to be used. The cantilever was extended with an extension segment (as shown in Fig. 3), in order to prevent device failure related to bending due to process-induced stresses. At the beginning of the etching, the etchant undercuts the tethers and begins to attack the area under the main cantilever, at the same time attacking the area under the release-control extensions. The dimensions of the structure should be designed based on detailed knowledge of the etchant to be used.

Acknowledgements

The authors would like to thank the Natural Science and Engineering Research Council of Canada (NSERC), and the Concordia-Seagram Fund for supporting this research. The assistance given by the Canadian Microelectronics Corporation (CMC) in fabricating these devices, through Mitel Corporation and the Can-MEMS collaboration, is also appreciated.

References

- 1 M. Parameswaran, H. P. Baltes, Lj. Ristic, A. C. Dhaded and A. M. Robinson: *Sensors and Actuators* **74** (1989) 289.
- 2 B. Nikpour, L. M. Landsberger, B. Haroun and M. Kahrizi: *Proc. of Canadian Conference on Electrical and Computer Engineering*, Calgary, Alberta, May 26–29 (1996) p. 80.
- 3 S. Naseh, L. M. Landsberger, M. Paranjape and M. Kahrizi: *Canadian Journal of Physics* **74**, Suppl. 1 (1996) S79.
- 4 S. Naseh: "Experimental Investigation of Anisotropic Etching of Silicon in Tetra-Methyl Ammonium Hydroxide," Thesis: Master of Applied Science, Concordia University (1995).
- 5 E. H. Klaassen, R. J. Reay, C. Storment, J. Audy, P. Henry, A. P. Brokaw and G. T. A. Kovacs: *Solid-State Sensor and Actuator Workshop*, Hilton Head, SC, June 2–6 (1996) p. 127.
- 6 A. Pandey, L. M. Landsberger, B. Nikpour, M. Paranjape and M. Kahrizi: "Experimental Investigation of High Si/Al Selectivity during Anisotropic Etching of Si{100} in TMAH," *Canadian Semiconductor Conference*, Ottawa ONT, Aug. 11–15, 1997.
- 7 A. Pandey, L. M. Landsberger, B. Nikpour, M. Paranjape and M. Kahrizi: *J. Vac. Sci. Technol. A* **16** (1998) 868.
- 8 H. Seidel, L. Csepregi, A. Heuberger and H. Baumgartel: *J. Electrochem. Soc.* **137** (1990) 3612.
- 9 I. H. Shames: *Mechanics of Deformable Solids* (Prentice-Hall, Englewood Cliff, N. J., 1964).
- 10 W. C. Tang, T. H. Nguyen, M. W. Judy and R. T. Howe: *Sensors and Actuators A* **21–23** (1990) 328.
- 11 K. E. Peterson: *Silicon as a Mechanical Material*, *Proc. IEEE*, Vol. 70, No. 5 (1982) p. 420.
- 12 P. J. French and A. G. R. Evans: *Solid State Electronics* **32** (1989) 1.